.

SPATIAL ADAPTIVITY APPLIED TO THE VARIATIONAL NODAL P_n EQUATIONS

Hui Zhang & E. E. Lewis
Northwestern University
Department of Mechanical Engineering
Evanston, IL 60208
e-lewis@northwestern.edu

ABSTRACT

A spatial adaptive grid method is presented for the solution of two-dimensional neutron transport problems employing the spherical harmonics method within the framework of the variational nodal method. The work represents the generalization of an approach previously applied to the neutron diffusion equation. After reviewing pertinent aspects of the derivation of the variational nodal response matrices, an a posteriori estimator of the local error in the scalar flux is developed. An iterative adaptive procedure is then presented and application made to two-dimensional problems. Results are presented for a P_5 solution of the well-known Iron-Water Benchmark Problem.

1. INTRODUCTION

Adaptive grid methods are widely used to increase the efficiency of finite element solid and fluid mechanics codes.[1] With these methods, relatively coarse spatial approximations are generated, and a criterion specified for the required local accuracy of the solution. The adaptive algorithm successively refines the local level of spatial approximation according to a a posteriori estimate of the local error until the local error criterion is met over the entire problem domain. Two classes of methods are employed. In *h* methods the spatial grid is refined by selectively subdividing finite elements. In *p* methods the element interfaces remain fixed, and the order of the trial functions is selectively increased to reduce local errors.

In an earlier work,[2] we formulated a *p* adaptive method to locally refine the spatial interface approximations in the variational nodal method. That formulation, however, was limited to the treatment of the diffusion approximation. Here we extended it to higher order P_n approximations. In the following section we outline the derivation of the variational nodal method (VNM) for the spherical harmonics equations, emphasizing only those aspects pertinent to the implementation of the adaptive method. In Section 3 we formulate a local error estimation techniques that is compatible with VNM P_n approximations and present the adaptive algorithm. In the final section we apply the method to a P_5 calculation of the well-known Iron-Water Benchmark Problem and evaluate the effectiveness of the results.

2. VARIATIONAL NODAL FORMULATION

The variational nodal formulation, treated in more detail elsewhere,[3-4] begins with the within-group, even-parity transport equation with isotropic scattering

$$-\hat{\Omega}\cdot\nabla\sigma^{-1}\hat{\Omega}\cdot\nabla\psi^{+}+\sigma\psi^{+}=\sigma_{s}\phi+S, \tag{1}$$

where s and s_s are the macroscopic total and scattering cross sections, and the scalar flux may be written in terms of the even-parity flux as

$$\phi=\int d\Omega\psi^{+}. \tag{2}$$

Equation (1) may be formulated as a variational principle in terms of a global functional, F, which is a superposition of volume and surface contributions from the V_n spatial hybrid finite elements (hereafter called nodes) comprising the problem domain

$$F[\psi^{+},\psi^{-}]=\sum_{v}F_{v}[\psi^{+},\psi^{-}], \tag{3}$$

where the contribution from node V_v with surface Γ_v is

$$F_{v}[\psi^{+},\psi^{-}]=\int_{v}dV\{\int d\Omega[\sigma^{-1}(\hat{\Omega}\cdot\nabla\psi^{+})^{2}+\sigma\psi^{+2}]-\sigma_{s}\phi^{2}-2\phi S\}+2\int_{\gamma}d\Gamma\int d\Omega\,\hat{n}\cdot\hat{\Omega}\psi^{+}\psi^{-}. \tag{4}$$

In the absence of the interface terms containing the odd-parity flux ψ^{-}, Eqs.(3) and (4) reduce to the functional that was first formulated by Vladimirov.[5] The use of ψ^{-} as a Lagrange multiplier at element interfaces gives rise to the primal hybrid finite element formulation referred to as the variational nodal method.

To reduce the functional to algebraic form, we approximate y^{+} within the node and ψ^{-} along the interfaces:

$$y^{+}(\vec{r},\hat{\Omega})\approx\mathbf{g}^{T}(\hat{\Omega})\otimes\mathbf{f}^{T}(\vec{r})\text{?}\qquad\vec{r}\in\mathbf{V}_{v} \tag{5}$$

$$f(\vec{r})\approx\mathbf{d}^{T}\otimes\mathbf{f}^{T}(\vec{r})\text{?},\qquad\vec{r}\in\mathbf{V}_{v} \tag{6}$$

and

$$y^{-}(\vec{r},\hat{\Omega})\approx\mathbf{h}^{T}(\vec{r})\otimes\mathbf{k}^{T}(\hat{\Omega})\text{?.}\qquad\vec{r}\in\Gamma_{v} \tag{7}$$

where $[\mathbf{d}]_i=d_{i1}$. The isotropic group source S is approximated by

$$S(\vec{r}) \approx \mathbf{d}^T \otimes \mathbf{f}^T(\vec{r})\mathbf{s}, \qquad \vec{r} \in \mathbf{V}_v \tag{8}$$

In the foregoing equations **?** and **?** are column vectors of unknown coefficients. The $\mathbf{f}(\vec{r})$ and $\mathbf{h}(\vec{r})$ are vectors of complete orthogonal polynomials of order p within the node and along the interfaces, respectively. They obey orthogonality relationships

$$\int_n dV \mathbf{f}(\vec{r})\mathbf{f}^T(\vec{r}) = V_n \mathbf{I} \tag{9}$$

and

$$\int_n d\Gamma \mathbf{h}(\vec{r})\mathbf{h}^T(\vec{r}) = \mathbf{I}. \tag{10}$$

The angular basis functions $\mathbf{g}(\hat{\Omega})$ and $\mathbf{k}(\hat{\Omega})$ are orthonormal even- and odd- parity spherical harmonics defined within the nodes and along the interfaces respectively.[4]

Inserting the expansions of ψ^+, ψ^- and S into Eq. (4) results in the reduced functional

$$F_v[\mathbf{?}, \mathbf{?}] = \mathbf{?}^? \mathbf{A} \mathbf{?} - 2\mathbf{?}^? \mathbf{s} + 2\mathbf{?}^? \mathbf{M} \mathbf{c}, \tag{11}$$

where the elements of the matrices **A** and **M** consist of space-angle integrals over the known trial functions.

To tailor the functional for use in adaptive methods, we make the following partitions. Let

$$\mathbf{?}^T = \left[\mathbf{?}_1^T, \mathbf{?}_2^T\right], \tag{12}$$

where $\mathbf{?}_1$ includes all of the spatial moments of the scalar flux, and $\mathbf{?}_2$ the moments of the higher-angular-order terms in the even-parity flux expansion. Likewise we partition the interface trial function

$$\mathbf{h}^T = [\mathbf{h}_a^T, \mathbf{h}_b^T], \tag{13}$$

where $\mathbf{h}_a$ includes only those polynomial terms through order p', where $p' < p$. There then exist a corresponding partition for the unknown coefficients at the interface:

$$\mathbf{?}^T = \left[\mathbf{?}_a^T, \mathbf{?}_b^T\right]. \tag{14}$$

Performing consistent partitioning of the **A** and **M** matrices we may rewrite Eq. (11) as

$$F_v[\mathbf{?}, \mathbf{c}] = \begin{bmatrix} \mathbf{?}_1 \\ \mathbf{?}_2 \end{bmatrix}^? \begin{bmatrix} \mathbf{A}_{11} & \mathbf{A}_{12} \\ \mathbf{A}_{21} & \mathbf{A}_{22} \end{bmatrix} \begin{bmatrix} \mathbf{?}_1 \\ \mathbf{?}_2 \end{bmatrix} - 2\begin{bmatrix} \mathbf{?}_1 \\ \mathbf{?}_2 \end{bmatrix}^? \begin{bmatrix} \mathbf{s}_1 \\ \mathbf{0} \end{bmatrix} + 2\begin{bmatrix} \mathbf{?}_1 \\ \mathbf{?}_2 \end{bmatrix}^? \begin{bmatrix} \mathbf{M}_{1a} & \mathbf{M}_{1b} \\ \mathbf{M}_{2a} & \mathbf{M}_{2b} \end{bmatrix} \begin{bmatrix} \mathbf{c}_a \\ \mathbf{c}_b \end{bmatrix}. \tag{15}$$

To formulate the adaptive grid method we first examine the spatial trial functions more closely. For two-dimensional Cartesian geometry, $\dim(\mathbf{f}) = (p+1)(p+2)/2$ since $\mathbf{f}$ is a complete polynomial of order p, and $\dim(\mathbf{h}) = 4(p+1)$ since we also take $\mathbf{h}$ to be a set of orthonormal polynomials of order p on each of the four interfaces. Taking $\mathbf{f}$ and $\mathbf{h}$ of the same order p results in an exact projection of the scalar flux distribution onto the nodal interfaces. However, the following computational procedures require that $\mathbf{M}$ be a full rank matrix, a condition that holds only if we take the interface spatial approximations to be of lower order $p' \le \max(p') < p$.[3] In this work we take p =6 for which $\max(p') = 4$.

In the above partition, the interface trial function is taken such that $\mathbf{h}_a$ consists of lower-order polynomials, which may have different values of p' on each interface, but everywhere meets the criterion $p' \le \max(p') = 4$. To account for this reduction in the functional, we simply delete $\boldsymbol{\psi}_b$ from the Lagrange multiplier, thereby reducing $\mathbf{h}$ to $\mathbf{h}_a$ and hence $\mathbf{M}$ to $\mathbf{M}_a$ in Eq. (15). The lower-order spatial interface approximation reduces the functional to

$$F_v[\boldsymbol{\psi}, \mathbf{c}_a] = \boldsymbol{\psi}^T \mathbf{A} \boldsymbol{\psi} - 2\boldsymbol{\psi}^T \mathbf{s} + 2\boldsymbol{\psi}^T \mathbf{M}_a \mathbf{c}_a . \tag{16}$$

where

$$\mathbf{M}_a = \begin{bmatrix} \mathbf{M}_{1a} \\ \mathbf{M}_{2a} \end{bmatrix}.$$

We may now proceed to obtain a set of response matrix equations for each nodal volume, from which we can solve for $\boldsymbol{\psi}$ and $\boldsymbol{\psi}_a$. Requiring the functional to be stationary with respect to a variation of the unknown coefficient vector $\boldsymbol{\psi}$ yields

$$\boldsymbol{\psi} = \mathbf{A}^{-1}\mathbf{s} - \mathbf{A}^{-1}\mathbf{M}_a \mathbf{c}_a . \tag{17}$$

The variation with respect to $\mathbf{c}_a$ across an interface leads to requirement that

$$\boldsymbol{\psi}_a = \mathbf{M}_a^T \boldsymbol{\psi} \tag{18}$$

be continuous across each interface Combining Eqs. (17) and (18), yields the even-parity interface flux moments in terms of the source moments within the node and the odd-parity flux moments on the interfaces:

$$\boldsymbol{\psi}_a = \mathbf{M}_a{}^T \mathbf{A}^{-1}\mathbf{s} - \mathbf{M}_a{}^T \mathbf{A}^{-1}\mathbf{M}\mathbf{c}_a . \tag{19}$$

To obtain the VNM form of the nodal response matrix, we make the transformation of variables,

$$\mathbf{j}^{\pm} = \tfrac{1}{4}\boldsymbol{\psi}_a \pm \tfrac{1}{2}\boldsymbol{\psi}_a, \tag{20}$$

which yields

$$\mathbf{j}^{+} = \mathbf{R}\mathbf{j}^{-} + \mathbf{B}\mathbf{s}, \tag{21}$$

where $\mathbf{R} = (\frac{1}{2}\mathbf{M}_a^T\mathbf{A}^{-1}\mathbf{M}_a + \mathbf{I})^{-1}(\frac{1}{2}\mathbf{M}_a^T\mathbf{A}^{-1}\mathbf{M}_a - \mathbf{I})$ and $\mathbf{B} = (\frac{1}{2}\mathbf{M}_a^T\mathbf{A}^{-1}\mathbf{M}_a + \mathbf{I})^{-1}\,\frac{1}{2}\mathbf{M}_a^T\mathbf{A}^{-1}$. Inserting Eqs. (20) into Eq. (17) then yields

$$\mathbf{?} = \mathbf{A}^{-1}\mathbf{s} - \mathbf{A}^{-1}\mathbf{M}_a(\mathbf{j}^{+} - \mathbf{j}^{-}). \tag{22}$$

3. ADAPTIVE METHOD

The adaptive method consists of locally refining the VNM approximations in successive iterations until a solution of acceptable accuracy is reached. To perform localized refinement, we must first formulate a local error estimate consistent with VNM that is calculable a posteriori. To accomplish this, we begin by defining the discretization error as the difference between the exact and approximate solution for element V_v

$$\varepsilon_v = \phi(\vec{r}) - \phi_a(\vec{r}), \qquad r \in V_v \tag{23}$$

Energy, stress and L^2 norms have most frequently served as a basis for local error indication.[1] The error in the L_2 norm for element V_v is defined as

$$\|\varepsilon_v\| = \sqrt{\int_v dV\left[\phi(\vec{r}) - \phi_a(\vec{r})\right]^2}\,, \tag{24}$$

where *v* refers to individual node V_v. Likewise, the scalar flux in the L_2 norm is

$$\|\phi_v\| = \sqrt{\int_v dV\phi^2(\vec{r})}\,. \tag{25}$$

The relative nodal error in the norm is defined by

$$\eta_v = \frac{\|\varepsilon_v\|}{\|\phi_v\|} \times 100\%, \tag{26}$$

or equivalently

$$\eta_v = \sqrt{\int_v dV[\phi\ (\vec{r}) - \phi_a(\vec{r})]^2 \Big/ \int_v d\Gamma\,\phi^2(\vec{r})} \times 100\%. \tag{27}$$

In practice, the exact solution of the problem is not available and a method to approximately evaluate the error must be devised. Zienkiewicz – Zhu (Z&Z) error estimator has been highly effective for spatial refinement of primal finite element calculations.[6,7] The essence of this error estimator is to use a more accurate estimate of

the solution $\phi_*(\vec{r})$ in place of the exact solution in the computation of the error. We may estimate the local relative error by replacing $f(\vec{r})$ with $\phi_*(\vec{r})$ in Eq.(27),

$$\eta_{*v} = \sqrt{\int_v dV[\phi_*(\vec{r}) - \phi_a(\vec{r})]^2 \Big/ \int_v dV \phi_*^2(\vec{r})} \times 100\%. \tag{28}$$

Obtaining a $\phi_*(\vec{r})$ that is close to the true ϕ in a computationally efficient manner is the key to the error estimation. The L_2 projection and averaging, superconvergent patch recovery (SPR) are widely used in solid mechanics to obtain $\phi_*(\vec{r})$.[6,7] In adaptive work applied to the spatial variables of S_n form of the neutron transport equation, errors have been estimated by using two successive iterates for $\phi_*(\vec{r})$ and $\phi_a(\vec{r})$.[8] This, however, requires the calculation to be carried out at two levels with uniform refinement before the first estimate can be made. In contrast, the following techniques for the VNM allow the first estimate of $\phi_*(\vec{r})$ to be made from the lowest order approximation, and then refined with each iterate.

The dimension of the VNM response matrix is the primary determinant of the number of degrees of freedom and of the CPU time. It is fixed by the odd-parity approximation **h** on the interface. Therefore, we require an a posteriori error estimate to determine where in the problem domain the nodal interface approximations should be further refined at each stage of the adaptive procedure. This must estimate the interface error in a manner that is compatible with the VNM. By integrating over a particular interface $\Gamma_{v\gamma}$ of node V_v instead of the volume integrals in Eq. (28) we have

$$h_{*g} = \sqrt{\int_{ng} d\Gamma[f_*(\vec{r})|_v - f_a(\vec{r})|_v]^2 \Big/ \int_{ng} d\Gamma f_*^2(\vec{r})|_v} \times 100\%. \tag{29}$$

There are, however, two neighboring nodes V_v that contribute to the interface between them. Therefore we let $\eta_{*\gamma}|_v$ and $\eta_{*\gamma}|_{v'}$ be the corresponding error contributions to the common interface and define

$$h_{*g} = \frac{1}{2}\left(h_{*g}|_v + h_{*g}|_{v'}\right) \times 100\%. \tag{30}$$

At boundaries, where there is no neighboring node $V_{v'}$, we use Eq.(29) directly.

We employ the following method to make the flux estimate $\phi_*(\vec{r})$. First note that the scalar flux distribution within the node may be deduced from Eqs (6) and (12) to be

$$f(\vec{r}) = \mathbf{f}^T(\vec{r})\mathbf{?}_1, \qquad \vec{r} \in \mathbf{V}_v. \tag{31}$$

Since **h** and **f** are the same order polynomial, we may project the flux distribution onto to the nodal interface to obtain the flux estimate $f_*(\vec{r})$ by using the orthonormal properties of **h** given in Eq. (10):

$$f_*(\vec{r}) = \mathbf{h}(\vec{r})^T \int_n d\Gamma \mathbf{h}(\vec{r}')\mathbf{f}^T(\vec{r}')\boldsymbol{\lambda}_1 \,. \qquad \vec{r} \in \Gamma_{ng} \tag{32}$$

Partitioning **h** as in Eq.(13) we may write

$$f_*(\vec{r}) = f_a(\vec{r}) + f_b(\vec{r}) = \mathbf{h}_a^T(\vec{r})\mathbf{f}_a + \mathbf{h}_b^T(\vec{r})\mathbf{f}_b, \qquad \vec{r} \in \Gamma_{ng} \tag{33}$$

where

$$\mathbf{f}_a = \int_{ng} d\Gamma \mathbf{h}_a(\vec{r}')\mathbf{f}^T(\vec{r}')\boldsymbol{\lambda}_1 \tag{34}$$

and

$$\mathbf{f}_b = \int_{ng} d\Gamma \mathbf{h}_b(\vec{r}')\mathbf{f}^T(\vec{r}')\boldsymbol{\lambda}_1 . \tag{35}$$

with the integrals taken over the interface $\Gamma_{v\gamma}$. Note that since only $\mathbf{h}_a$ is used in the Lagrange multiplier, only the moments $\mathbf{f}_a$ are included as components of the vector $\boldsymbol{\lambda}_a$ which is forced to be continuous across the interfaces. Thus $f_a(\vec{r})$ is continuous across the nodal interfaces, but $f_b(\vec{r})$ is not. The interfacial discontinuities as measured by the magnitudes of $f_b(\vec{r})$ thus provide us with a measure of the local error in the solution.

Utilizing Eq. (33) and the orthonormal properties of **h,** we may write Eq.(29) as

$$h_{*g} = \sqrt{\mathbf{f}_b^T \mathbf{f}_b \,/\, \mathbf{f}_*^T \mathbf{f}_*} \times 100\,\%, \tag{36}$$

were

$$\mathbf{f}_* = \int_{ng} d\Gamma \mathbf{h}(\vec{r}')\mathbf{f}^T(\vec{r}')\boldsymbol{\lambda}_1 . \tag{37}$$

To determine the efficacy of the estimate, we would like to determine how close it comes to Eq. (29) when $f_*(\vec{r})$ is replaced by the exact scalar flux. Unfortunately, there are few problems for which the exact solution is known. Instead we obtain a reference solution $f_r(\vec{r})$ numerically. We do this by taking p' = Max(p) = 4 on all of the elemental interfaces. We denote the fourth order reference solution trial functions by $\mathbf{h}_r$ and the reference flux moments by $\boldsymbol{\lambda}_{1r}$ and $\mathbf{f}_r$ so that

$$f_r(\vec{r}) - f_a(\vec{r}) = \mathbf{h}_r^T(\vec{r})\mathbf{f}_r - \mathbf{h}_a^T(\vec{r})\mathbf{f}_a . \tag{38}$$

Thus substituting $f_r(\vec{r})$ for $f_*(\vec{r})$ in Eq. (29) we obtain, after some algebra,

$$h_{rg} = \sqrt{(\mathbf{f}_r^T \mathbf{f}_r + \mathbf{f}_a^T \mathbf{f}_a - 2[\mathbf{f}_a^T, \mathbf{0}^T]\mathbf{f}_r) \,/\, \mathbf{f}_r^T \mathbf{f}_r} \times 100\,\% . \tag{39}$$

Finally we would like to know not only how well Eq.(36) approximates Eq.(39), but also how well the surface integrals that resulted in Eq.(39) approximate the volume

integral in Eq. (27), since it is the error in the reaction rates that is of most interest in neutronics calculations. To do this we use the scalar flux coefficients $\mathbf{?}_1$ and $\mathbf{?}_{1r}$ obtained from the approximate and reference calculation respectively in Eq. (27) to obtain

$$h_{rv} = \sqrt{(\mathbf{?}_{1r} - \mathbf{?}_1)^T (\mathbf{?}_{1r} - \mathbf{?}_1) / \mathbf{?}_{1r}^T \mathbf{?}_{1r}} \times 100\% . \tag{40}$$

To complete the comparison, we average Eqs. (36) and (39) over the four nodal interfaces, in order to make the nodal comparisons with Eq. (40). From Eq. (39),

$$\hat{h}_{rn} = \frac{1}{4} \sum_{g=1}^{4} h_{rg} , \tag{41}$$

and similarly from Eq.(36)

$$\hat{h}_{*_n} = \frac{1}{4} \sum_{g=1}^{4} h_{*_g} . \tag{42}$$

In summary, Eq.(36), and its nodal average Eq. (42), are used in the adaptive procedure. For the techniques to be valid, however, the relative magnitudes of the local error given by Eq. (42) must approximate those given by Eq. (41); and those given by Eq. (41) must in turn reasonably approximate those of Eq. (40). Since Eq. (40) represents the error in the volumetric average of the flux and therefore in reaction rates, it is the primary quantity that we want to minimize. Numerical experiments on a number of problems both in diffusion and P_n theory indicate that these estimates agree sufficiently well that the foregoing error estimate is valid. The agreement is illustrated in the following section.

The adaptive iteration proceeds as follows. We initiate the procedure by performing the lowest-order calculation (n=0) with p'=1 on all interfaces. We then calculate the resulting h_{*_g} from Eq. (30) at each interface. If for a particular interface

$$h_{*_g} > \frac{1}{3} Max(h_{*_g})$$

then $p' \rightarrow p' + 1$ on that interface until either p'=4 or $h_{*_g} < h_0$ where h_0 is a termination criterion.

4. ILLUSTRATIVE EXAMPLE

To illustrate the adaptive method for spherical harmonics approximations we apply it in the P_5 approximation to the well-known Iron-Water Benchmark problem. The cross sections for the one-group configuration shown in Figure 1 are given elsewhere.[9] The problem domain is composed of a source region at the center of a water pool that is surrounded in turn by an iron shield and by an outer water region. A 10x10 nodal grid is applied to the 30-cm square.

In Figure 2 are shown the three estimators, h_{rv}, $\hat{h}_{rn}$ and $\hat{h}_{*_n}$ given by Eqs. (40), (41) and (42). In these Figures, the approximate solution is the initial case where $p'=1$ on all interfaces. While there are some differences, the similarity in the topology of the three plots indicates that the estimated interface error does provide a reasonable estimate of the error in the volume average of the nodal flux.

Figure 3 shows the spatial distributions of the error indicator $\hat{h}_{*_n}$ at each iteration of the adaptive process. Note the successive attenuation of the local error at each iteration indicating the convergence toward the reference solution. Finally, we compare the savings in computational effort achieved with the adaptive method by examining the number of interface degrees of freedom vs. the maximum interface error at each iteration of the adaptive method. We compare this to the same quantities for a calculation in which p' the degree of the interface polynomials is increased uniformly over the entire problem domain. As indicated in Figure 4, the adaptive method reduces substantially the number of degrees of freedom and therefore the CPU time required to achieve a given level of local error in the solution.

REFERENCES

1. O. C. Zienkiewicz and R. L Taylor, *The Finite Element Method*, Fourth Edition, Vol 1, McGraw-Hill, New York (1990).

2. Hui Zhang and E. E. Lewis, "An Adaptive Approach to Variational Nodal Diffusion Problems," *Nucl. Sci. Eng*. **137**, 14 (2001).

3. G. Palmiotti, E. E. Lewis, C. B. Carrico, "VARIANT: VARIational Anisotropic Nodal Transport for Multidimensional Cartesian and Hexagonal geometry Calculation, Argonne National Laboratory ANL-95/40 (1995).

4. E. E. Lewis, C. B. Carrico, G. Palmiotti, "Variational Nodal formulation of the Spherical Harmonics equations," *Nucl. Sci. Eng*. **122**, 194 (1996).

5. V. S. Vladimirov, "Mathematical Problems in the One-Velocity Theory of Particle Transport," Atomic Energy of Canada Ltd. (1963) (translated from *Trans. V.A.Steklov Mathematical Institute*, **61**, 1961)

6. O. C. Zienkiewicz and J. Z. Zhu, "Superconvergent recovery technique and a posteriori error estimators", *Int. J. Numer. Method Eng.* **30**, pp. 1331-1364 (1992).

7. O. C. Zienkiewicz and J. Z. Zhu, "A posteriori error estimation and the three-dimensional automatic mesh generation", *Finite Elements in Analysis and Design* **25**, pp. 167-184 (1997).

8. O. M. Zamonsky, C. J. Gho, Y. Y. Asmy, "Error Estimatoion and Adaptive Order Nodal Method for Solving Multidimensional Transport Problems," *Proc Tpl Mtg. Radiation and Shielding*, Nashville, TN, April 19-23, 1998 Am. Nucl. Soc. (1998).

9. H. Khalil, "A Nodal diffusion technique for Synthetic Acceleration of Nodal Sn Calculations," *Nucl. Sci. Eng.*, **90**, 263 (1985).

ACKNOWLEDGEMENT

This work was supported in part by DOE- LANL Award #11152-00-23

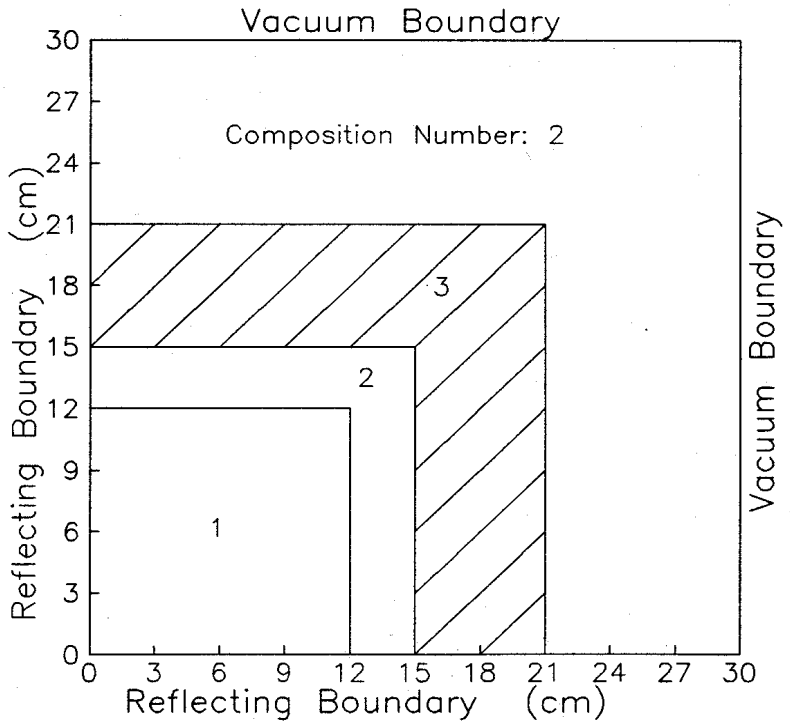

Fig. 1 Iron-Water Benchmark Problem

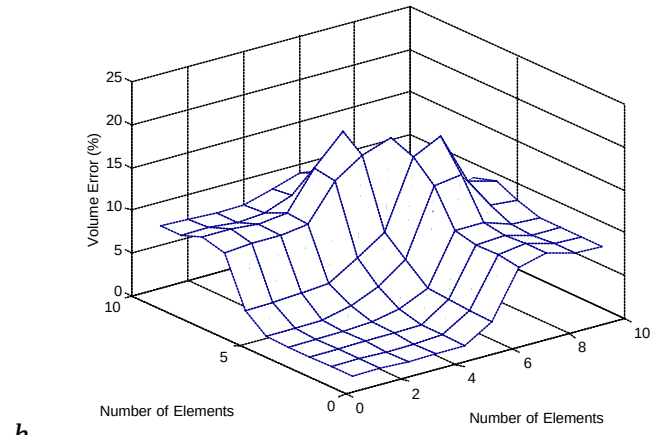

h_{rv}

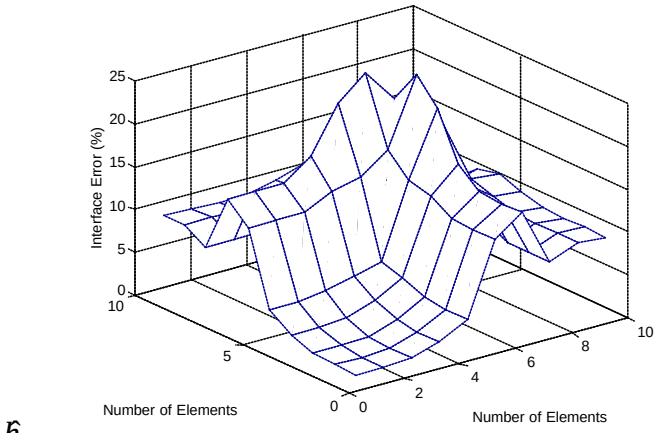

$\hat{h}_{rn}$

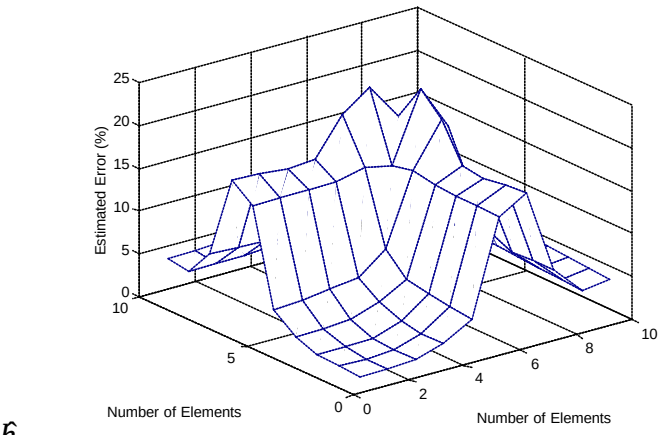

$\hat{h}_{*n}$

Figure 2 Comparison among h_{rv}, $\hat{h}_{rn}$ and $\hat{h}_{*n}$, the volume error, interface error and estimated error in P_5 approximation for the Iron-Water Benchmark Problem

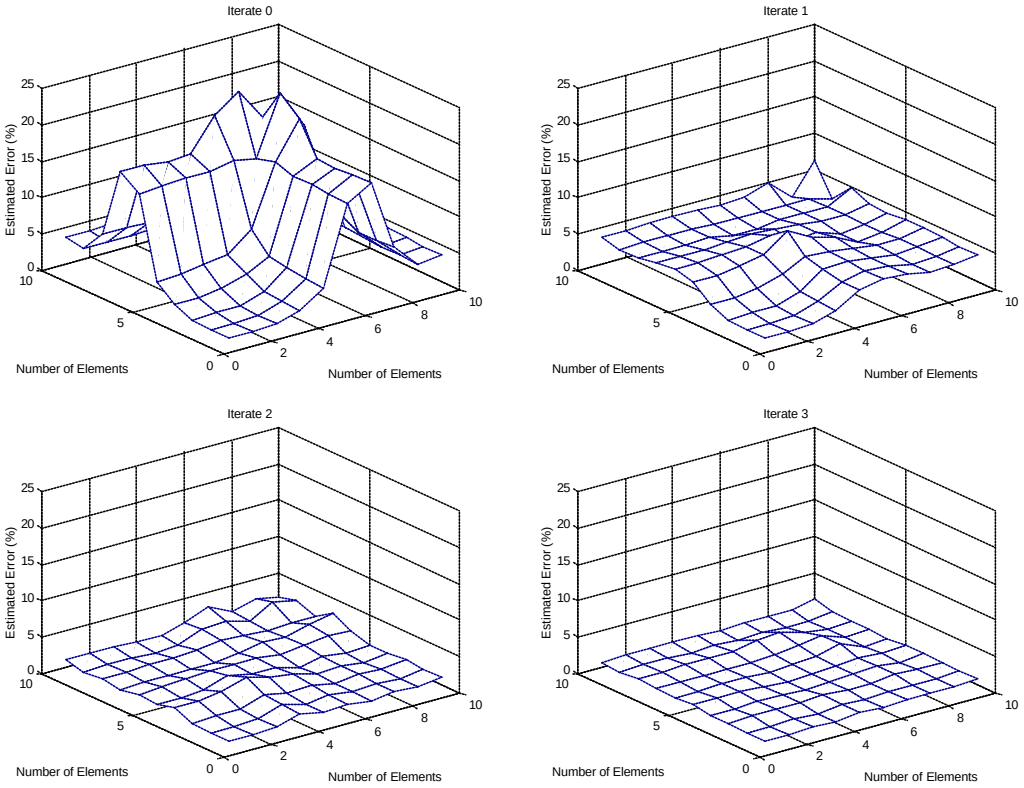

Figure 3 Error following each adaptive iteration in P_5 approximation for the Iron-Water Benchmark Problem

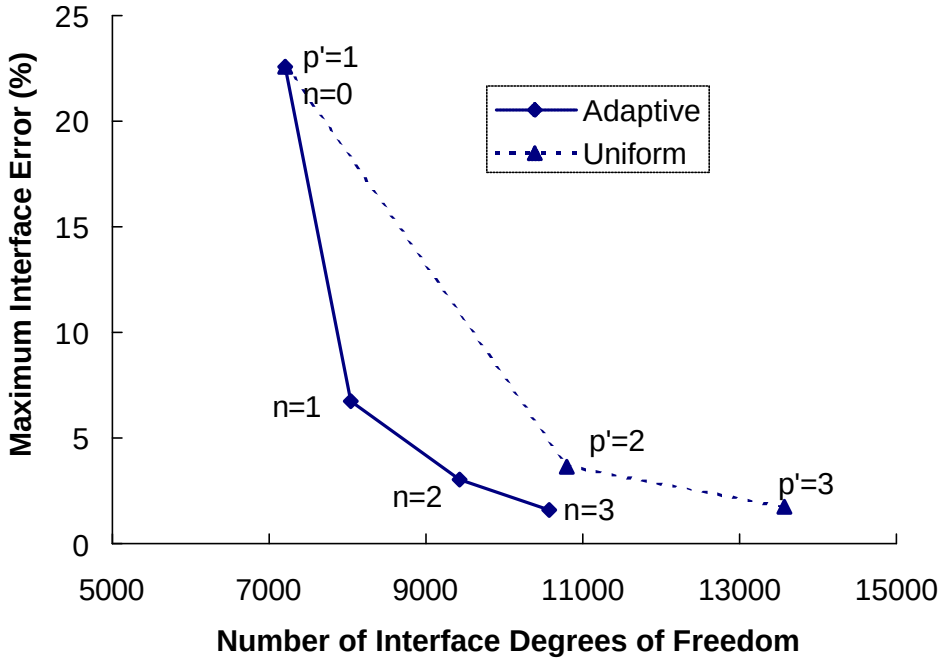

Figure 4. Maximum interfaace error comparison between spatial adaptive and uniform refinement methods in P_5 approximation for the Iron-Water Benchmark Problem